Fixation probabilities of evolutionary coordination games on two coupled populations

Liye Zhang, Limin Ying, Jie Zhou, Shuguang Guan, and Yong Zou*
Department of Physics, East China Normal University, Shanghai, 200062, China
(Received 12 April 2016; published 12 September 2016)

Evolutionary forces resulted from competitions between different populations are common, which change the evolutionary behavior of a single population. In an isolated population of coordination games of two strategies (e.g., s_1 and s_2), the previous studies focused on determining the fixation probability that the system is occupied by only one strategy (s_1) and their expectation times, given an initial mixture of two strategies. In this work, we propose a model of two interdependent populations, disclosing the effects of the interaction strength on fixation probabilities. In the well-mixing limit, a detailed linear stability analysis is performed, which allows us to find and to classify the different equilibria, yielding a clear picture of the bifurcation patterns in phase space. We demonstrate that the interactions between populations crucially alter the dynamic behavior. More specifically, if the coupling strength is larger than some threshold value, the critical initial density of one strategy (s_1) that corresponds to fixation is significantly delayed. Instead, the two populations evolve to the opposite state of all (s_2) strategy, which are in favor of the red queen hypothesis. We delineate the extinction time of strategy (s_1) explicitly, which is an exponential form. These results are validated by systematic numerical simulations.

DOI: 10.1103/PhysRevE.94.032307

I. INTRODUCTION

Evolutionary game theory helps to explain the characteristic interaction patterns of a population of individuals [1,2]. In a population of coordination games of two strategies, one central problem is to disclose the striking properties of fixation, which refers to the probability for one strategy to take over the entire population, causing the extinction of the other strategy [3]. For example, suppose that there are two strategies, cooperation and defection, in a population of size N, the quantity of interest in this evolutionary process is the fixation probability of cooperators, i.e., the probability to end up in a state with N cooperators given that the initial number of cooperators is n. When the initial number of cooperators is larger than n_0, the system reaches a state of population-wide of only cooperators, while on the other hand, the system reaches a state of all defectors if the initial number of cooperators is smaller than n_0. Certainly, it is necessary to determine the critical initial density of cooperators $x_0 = n_0/N$ that separates the two absorbing states of the system and the corresponding expectation times. Traditionally, when the population is homogeneously well mixed and of infinite size ($N \to \infty$), the system is essentially described by deterministic replicator equations, which determine the direction and velocity of the evolutionary dynamics [2].

However, large deviations have been observed in numerical simulations due to finite-size effects [4,5], or heterogeneous interaction patterns between players [6,7]. Evolutionary dynamics in populations of finite sizes are essentially stochastic, which require stochastic tools to describe these phenomena [8–15]. Comparing to the continuous representations of the evolutionary dynamics by replicator equations, stochastic approach considers the state space of the system as discrete and determines into which direction the system will evolve with certain probabilities. More importantly, a stochastic modeling considers explicitly the microscopic mechanisms that govern the transmission of strategies from one player to another in terms of various selection dynamics, for instance, pairwise comparison processes, Moran process, and Wright-Fisher process. Therefore, stochastic frameworks have provided many insights on the microscopic properties of the dynamic process of fixations [3–5,16–18]. Different implementations of strategy updating rules make the fixation properties fairly complicated, including selecting strength [19,20] and imitation- and aspiration-driven dynamics [21]. Furthermore, population structures and spatial constraints have influences on the strategy-spreading dynamics [22–27] as well. Simulations of this dynamic process on populations of complex network structures show large deviations from the theoretical predictions by replicator equations, which further demonstrate the usefulness of stochastic tools [28].

So far most studies on the dynamic processes of fixations have concentrated on a single population [5,28]. However, in most cases of biological or social systems, the population is not isolated, instead, interactions between populations often take place at different levels according to different rules [29]. In general, when two populations interact with each other, nontrivial co-evolutionary dynamics will take place in many different contexts. For instance, in evolutionary biology, the red queen hypothesis has been proposed to explain the situation that every improvement in one species will lead to a selective advantage for that species, but it gets a competitive advantage on the other species over certain temporal and geographic scales [30,31]. This means that fitness increase in one population will tend to lead to fitness decrease in the other population, yielding complex interaction patterns [32]. Concerning evolutionary game dynamics on interdependent populations, many novel phenomena that would not be present in a single population have been recently shown [33–35]. To a large extent, it should be expected that the rules governing one population do not necessarily play the same roles as for two or more populations, since competitions exist among interacted populations. In the particular case of fixation process, it remains largely unclear how population interaction strengths change the fixation probabilities and their corresponding fixation times.

*yzou@phy.ecnu.edu.cn

In a single population of two strategies, s_1 and s_2 (where each individual plays a coordination game with its counterpart), the quantity of interest is to study the density of individuals adopting the strategy s_1, which is denoted by x, while the density of individuals of strategy s_2 is $1-x$. There are two absorbing states: (i) one absorbing state corresponds to all players are of pure s_1 strategy, i.e., $x=1$; and (ii) the second absorbing state is $x=0$, i.e., all players have s_2 strategy. As replicator equation predicts, the system exhibits bistability, which shows discontinuity at $x^* \in (0,1)$ separating the absorbing state $x=0$ from $x=1$. Given an initial density x of s_1 strategy at time t_0, the system eventually will be absorbed at any of the two boundary states with probability 1. For an initial frequency above x^*, the population evolves toward 100% of pure s_1 individuals [4,10]. Certainly, the estimation of the critical value of x^* is an important issue and has been recently discussed in detail in Ref. [28], especially when dealing with structured populations of finite sizes. What would happen to the value x^* if another population is present? Here, we propose a coordination game model on two coupled populations, focusing on the roles of population interactions. With detailed theoretical analysis and substantial numerical simulations, we find that the value x^* will be significantly delayed in the presence of selection pressure exerted by the other population. Furthermore, we find a regime where the population shows red queen dynamic scenario, namely, the system is attracted to the opposite state of pure s_2 players provided with sufficiently strong coupling strength.

The structure of this paper is organized as follows: We present the game model in Sec. II and the equations governing the dynamics are derived in Sec. III. In Sec. IV, we obtain the fixed points of the system and their respective stability properties. The theoretical analysis will be validated by numerical simulations in Sec. V, where we find red queen dynamic behavior. In Sec. VI, we come to the conclusions.

II. GAME MODEL

Consider two populations P and Q. In each population there are N players and each player has two options for strategy s_1 and s_2. In the case of well-mixed populations, a pair of two connected players in population P (respectively, in Q) play a symmetric game and the payoff matrix $\mathbf{A}_P$ (respectively, $\mathbf{A}_Q$) are expressed as

$$\mathbf{A}_P = \begin{pmatrix} a & b \\ c & d \end{pmatrix}, \ \mathbf{A}_Q = \begin{pmatrix} A & B \\ C & D \end{pmatrix}. \tag{1}$$

Depending on the choice of the payoff matrices $\mathbf{A}_P$ and $\mathbf{A}_Q$, one implements different game models. In this work, we choose $a > c, d > b$ $(A > C, D > B)$ in both matrices such that we have coordination games with bistability in each system [5]. At time step t, we assume there are i out of N players in P having s_1 strategy and correspondingly there are j out of N players in Q having s_1 strategy. If the two populations P and Q are independent, the payoffs of each strategy are the following:

$$\begin{aligned} u_{s_1}^P &= ai + b(N-i), \\ u_{s_2}^P &= ci + d(N-i), \\ u_{s_1}^Q &= Aj + B(N-j), \\ u_{s_2}^Q &= Cj + D(N-j), \end{aligned} \tag{2}$$

where the superscripts represent the group P and Q, respectively.

The interaction between P and Q influences the individual's payoffs and hence fitness. In this work, we assume that the payoff of one player is determined by the actions between its opponent and itself. Therefore, we use the coupling parameter λ to quantify the interacting information between populations. More specifically, the payoffs of each strategy read

$$\begin{aligned} u_{s_1}^P &= [ai + b(N-i)] + \lambda_P[aj + b(N-j)], \\ u_{s_2}^P &= [ci + d(N-i)] + \lambda_P[cj + d(N-j)], \\ u_{s_1}^Q &= [Aj + B(N-j)] + \lambda_Q[Ai + B(N-i)], \\ u_{s_2}^Q &= [Cj + D(N-j)] + \lambda_Q[Ci + D(N-i)], \end{aligned} \tag{3}$$

where $\lambda_{P,Q} \geqslant 0$ and $\lambda_P \neq \lambda_Q$ are the coupling parameters. Putting it differently, λ_P can be regarded as the sensitivity of a player in population P to the information that it collects from the group Q (λ_Q can be interpreted in a full analogy). Furthermore, $\lambda_{P,Q}$ can be understood as considering the influence of migration rates on the stochastic dynamics of subdivided populations [36–39]. We define the frequency of s_1 players in P and Q as $x = i/N$ and $y = j/N$. When N is sufficiently large, the payoffs of each strategy [Eqs. (3)] are rewritten as

$$\begin{aligned} u_{s_1}^P &= N\{[ax + b(1-x)] + \lambda_P[ay + b(1-y)]\}, \\ u_{s_2}^P &= N\{[cx + d(1-x)] + \lambda_P[cy + d(1-y)]\}, \\ u_{s_1}^Q &= N\{[Ay + B(1-y)] + \lambda_Q[Ax + B(1-x)]\}, \\ u_{s_2}^Q &= N\{[Cy + D(1-y)] + \lambda_Q[Cx + D(1-x)]\}. \end{aligned} \tag{4}$$

By definition, it is assumed that fitness of a strategy is a monotonically increasing function of its payoff, i.e., $f_{s_1}^P \equiv f_{s_1}^P(u_{s_1}^P)$, $f_{s_2}^P \equiv f_{s_2}^P(u_{s_2}^P)$, $f_{s_1}^Q \equiv f_{s_1}^Q(u_{s_1}^Q)$, and $f_{s_2}^Q \equiv f_{s_2}^Q(u_{s_2}^Q)$. There are several alternative functions in representing fitness. In general, the most commonly adopted one is the linear fitness function $f = 1 - \hat{\beta} + \hat{\beta}u$, where f denotes fitness, u is the average payoff, and $\hat{\beta}$ is selection strength [40]. However, the selection strength $\hat{\beta}$ cannot exceed a threshold $\hat{\beta}_{\max}$ because of negative fitness, which is typical for frequency-dependent Moran processes. In order to obtain results with any higher selection strengths, in this work, we apply an exponential fitness function $f = e^{\beta u}$ [6,40,41]. More specifically, $f_{s_1}^P \equiv \exp(\beta u_{s_1}^P)$, $f_{s_2}^P \equiv \exp(\beta u_{s_2}^P)$, $f_{s_1}^Q \equiv \exp(\beta u_{s_1}^Q)$, and $f_{s_2}^Q \equiv \exp(\beta u_{s_2}^Q)$. Note that the selection strength β has an order of population size N in comparison to $\hat{\beta}$, namely $\hat{\beta} = \beta/N$, which was often used in the literature based on the average payoffs [5,19].

When considering two populations of unequal sizes $N_P \neq N_Q$, one can introduce a parameter $\alpha = N_P/N_Q$ in Eqs. (4) as has been done in Refs. [33,42]. In our model, this could be implemented by two different selection strength β_P, β_Q provided the assumption that fitness of a strategy is a monotonic function of its payoff is fulfilled. In this work, we consider the case of equal population sizes, yet with rich

dynamics. The study of a more general case of $N_P \neq N_Q$ will be a subject of future work.

III. TRANSITION PROBABILITIES

We consider each population, respectively, undergoes the *Moran process:* Suppose at time t, there are i and j players in P and Q having action s_1. At time t, one of player X in P is chosen proportional to its fitness. This chosen individual produces one identical offspring. To keep the population size N constant, a randomly chosen individual X' in P is removed from the population before the offspring is added [5,10]. This birth-death process is repeated for population Q, separately.

In the next time step $t+1$, the transition probability that the number of s_1 players is increased to $i+1$ in P (respectively, $j+1$ in Q) can be expressed as

$$T_+^P = \frac{N-i}{N} \cdot \frac{f_{s_1}^P \cdot i}{f_{s_1}^P \cdot i + f_{s_2}^P \cdot (N-i)}, \tag{5}$$

$$T_+^Q = \frac{N-j}{N} \cdot \frac{f_{s_1}^Q \cdot j}{f_{s_1}^Q \cdot j + f_{s_2}^Q \cdot (N-j)}. \tag{6}$$

Replacing $x = i/N, y = j/N$ (proportions of populations playing s_1 strategy in P and Q, respectively), we obtain

$$T_+^P = (1-x)\frac{f_{s_1}^P x}{f_{s_1}^P x + f_{s_2}^P (1-x)} = x(1-x)\frac{f_{s_1}^P}{\bar{f}^P}, \tag{7}$$

$$T_+^Q = (1-y)\frac{f_{s_1}^Q y}{f_{s_1}^Q y + f_{s_2}^Q (1-y)} = y(1-y)\frac{f_{s_1}^Q}{\bar{f}^Q}, \tag{8}$$

where $\bar{f}^P = f_{s_1}^P x + f_{s_2}^P (1-x)$ and $\bar{f}^Q = f_{s_1}^Q y + f_{s_2}^Q (1-y)$ characterize the average fitness of group P and Q, respectively. In a fully analogy, the transition probabilities that the number of s_1 players is reduced to $i-1$ in P (respectively, $j-1$ in Q) are

$$T_-^P = x(1-x)\frac{f_{s_2}^P}{\bar{f}^P}, \tag{9}$$

$$T_-^Q = y(1-y)\frac{f_{s_2}^Q}{\bar{f}^Q}. \tag{10}$$

The probabilities to keep i s_1 players in P unchanged is $T_0^P = 1 - T_+^P - T_-^P$, respectively, in Q we have $T_0^Q = 1 - T_+^Q - T_-^Q$.

When $N \to \infty$, the evolutionary dynamics of the strategy densities are determined by the following two-dimensional replicator equations:

$$\frac{dx}{dt} = F = T_+^P - T_-^P = x(1-x)\frac{f_{s_1}^P - f_{s_2}^P}{\bar{f}^P}, \tag{11}$$

$$\frac{dy}{dt} = G = T_+^Q - T_-^Q = y(1-y)\frac{f_{s_1}^Q - f_{s_2}^Q}{\bar{f}^Q}. \tag{12}$$

In this coupled system, we have the phase plane of unit square $[0,1] \times [0,1]$.

Note that, for coordination games [$(a > c, d > b)$ and $(A > C, D > B)$] on two independent populations P and Q ($\lambda_{P,Q} = 0$), we recover the results that have been reported in Ref. [5]. More specifically, the replicator equation shows that there are trivial equilibria points $\hat{x} = 0$ and $\hat{x} = 1$ and an unstable fixed points x^* in P (respectively, $\hat{y} = 0$, $\hat{y} = 1$, and y^* in Q), where x^* and y^* read

$$x^* = \frac{d-b}{a+d-b-c}, \tag{13}$$

$$y^* = \frac{D-B}{A+D-B-C}, \tag{14}$$

where $0 < x^*, y^* < 1$. The ratios between x^* and y^* for two uncoupled populations are further denoted by

$$\varepsilon_1 = \frac{y^*}{x^*}, \quad \varepsilon_2 = \frac{1-y^*}{1-x^*}. \tag{15}$$

It turns out that ε_1 and ε_2 are helpful for bifurcation analysis as shown below.

IV. FIXED POINTS AND STABILITIES

The fixed points of the two coupled populations [Eqs. (11) and (12)] are determined by $F = dx/dt = 0$ and $G = dy/dt = 0$, which yield nine fixed points: (0,0), (0,1), (1,0), (1,1), $(x^L(0),0)$, $(x^L(1),1)$, $(0,y^L(0))$, $(1,y^L(1))$, and $(x^\sharp, y^\sharp)$. It is an easy task to obtain fixed points (0,0), (0,1), (1,0), and (1,1), but it is more complicated to obtain $(x^L(0),0)$, $(x^L(1),1)$, $(0,y^L(0))$, $(1,y^L(1))$, and $(x^\sharp, y^\sharp)$, which will be discussed in detail below.

We start by providing a geometrical method to obtain fixed points of the system. We first consider the quasisteady (marginal) state of the system, namely $F = 0, G \neq 0$ as an example. The x nullcline is defined by $F = 0$, which yields three solutions, $x = 0, x = 1$, and the third implicit solution of $f_{s_1}^P = f_{s_2}^P$. The assumption that fitness is a monotonically increasing function of the payoff leads to $u_{s_1}^P = u_{s_2}^P$, namely,

$$\begin{aligned} &ax + b(1-x) + \lambda_P[ay + b(1-y)] \\ &\quad = cx + d(1-x) + \lambda_P[cy + d(1-y)]. \end{aligned} \tag{16}$$

Thus, the x nullcline is simplified as

$$x^L(y) = \frac{(d-b)(1+\lambda_P)}{a+d-b-c} - \lambda_P y = x^* + \lambda_P(x^* - y), \tag{17}$$

where $0 \leqslant x^L(y), y \leqslant 1$. It is certain that $x^L = x^*$ when $\lambda_P = 0$. The x nullcline [Eq. (17)] characterizes the influence of population Q on the fixed point x^* of population P and the interpretation is rather straightforward:

(1) The quasisteady state x^L of population P is a linear function of y.

(2) For $\lambda_P > 0$, the contribution of the density y of Q is to change the position of x^*. More specifically, we have $x^L > x^*$ if $y < x^*$, while $x^L < x^*$ if $y > x^*$.

(3) For any given density y of population Q, the quasisteady state x^L depends on the position of x^* and λ_P, while independent of the payoff matrix Q and λ_Q.

In a full analogy, the y-nullcline $y^L(x)$ (defined by $F \neq 0$, $G = 0$) is as follows:

$$y^L(x) = \frac{(D-B)(1+\lambda_Q)}{A+D-B-C} - \lambda_Q x = y^* + \lambda_Q(y^* - x), \tag{18}$$

where $0 \leqslant x, y^L(x) \leqslant 1$. Furthermore, $y^L(x)$ has the same properties as $x^L(y)$.

TABLE I. Entries of the Jacobian matrix [Eq. (19)].

Fixed point	$\bar{f}^P \frac{\partial F}{\partial x}$	$\bar{f}^P \frac{\partial F}{\partial y}$	$\bar{f}^Q \frac{\partial G}{\partial x}$	$\bar{f}^Q \frac{\partial G}{\partial y}$
(0,0)	$(f^P_{s_1} - f^P_{s_2})\|_{(0,0)}$	0	0	$(f^Q_{s_1} - f^Q_{s_2})\|_{(0,0)}$
(0,1)	$(f^P_{s_1} - f^P_{s_2})\|_{(0,1)}$	0	0	$-(f^Q_{s_1} - f^Q_{s_2})\|_{(0,1)}$
(1,0)	$-(f^P_{s_1} - f^P_{s_2})\|_{(1,0)}$	0	0	$(f^Q_{s_1} - f^Q_{s_2})\|_{(1,0)}$
(1,1)	$-(f^P_{s_1} - f^P_{s_2})\|_{(1,1)}$	0	0	$-(f^Q_{s_1} - f^Q_{s_2})\|_{(1,1)}$
$(x^L(0),0)$	$x^L(0)[1-x^L(0)]$ $\eta_1(a+d-b-c)$	$\lambda_P x^L(0)[1-x^L(0)]$ $\eta_1(a+d-b-c)$	0	$(f^Q_{s_1} - f^Q_{s_2})\|_{(x^L(0),0)}$
$(x^L(1),1)$	$x^L(1)[1-x^L(1)]$ $\eta_2(a+d-b-c)$	$\lambda_P x^L(1)[1-x^L(1)]$ $\eta_2(a+d-b-c)$	0	$-(f^Q_{s_1} - f^Q_{s_2})\|_{(x^L(1),1)}$
$(0,y^L(0))$	$(f^P_{s_1} - f^P_{s_2})\|_{(0,y^L(0))}$	0	$\lambda_{Qy^L}(0)[1-y^L(0)]$ $\eta_3(A+D-B-C)$	$(y^L(0)[1-y^L(0)]$ $\eta_3(A+D-B-C)$
$(1,y^L(1))$	$-(f^P_{s_1} - f^P_{s_2})\|_{(1,y^L(0))}$	0	$\lambda_{Qy^L}(1)[1-y^L(1)]$ $\eta_4(A+D-B-C)$	$y^L(1)[1-y^L(1)]J$ $\eta_4(A+D-B-C)$
$(x^\sharp, y^\sharp)$	$x^\sharp[1-x^\sharp]C$ $\eta_5(a+d-b-c)$	$\lambda_P x^\sharp[1-x^\sharp]$ $\eta_5(a+d-b-c)$	$\lambda_Q y^\sharp[1-y^\sharp]$ $\eta_6(A+D-B-C)$	$y^\sharp[1-y^\sharp]I$ $\eta_6(A+D-B-C)$

When nullclines $x^L(y)$ and $y^L(x)$ cross the boundaries of the unit square $[0,1]\times[0,1]$, we have fixed points of $(x^L(0),0)$, $(x^L(1),1)$, $(0,y^L(0))$, $(1,y^L(1))$, and the intersection of $x^L(y)$ and $y^L(x)$ yields $(x^\sharp, y^\sharp)$. We emphasize the different notations between $(x^\sharp, y^\sharp)$ and x^*, y^* [Eqs. (13) and (14)].

The stability of the fixed points is determined by the Jacobian matrix

$$J = \begin{pmatrix} \frac{\partial F}{\partial x} & \frac{\partial F}{\partial y} \\ \frac{\partial G}{\partial x} & \frac{\partial G}{\partial y} \end{pmatrix}. \tag{19}$$

The particular expressions for the entries of Eq. (19) are provided in TableI (Appendix A). We further denote the determinant and trace of the matrix as

$$\Delta = \frac{\partial F}{\partial x}\frac{\partial G}{\partial y} - \frac{\partial F}{\partial y}\frac{\partial G}{\partial x}, \tag{20}$$

$$T = \frac{\partial F}{\partial x} + \frac{\partial G}{\partial y}. \tag{21}$$

Therefore, the necessary and sufficient conditions for a fixed point being stable is $\Delta > 0$ and $T < 0$. A fixed point is called a saddle point if $\Delta < 0$. For the purpose of convenience, we make the following notations:

$$\lambda_P^{c_1} = \frac{d-b}{a-c}, \quad \lambda_Q^{c_1} = \frac{A-C}{D-B}, \qquad \lambda_P^{c_2} = \frac{a-c}{d-b}, \quad \lambda_Q^{c_2} = \frac{D-B}{A-C}. \tag{22}$$

Therefore, we evaluate the stability conditions for each fixed point in the following.

A. Fixed points (0,0) and (1,1)

It is easy to show that the following terms are negative:

$$\left(f^P_{s_1} - f^P_{s_2}\right)\Big|_{(0,0)}, \left(f^Q_{s_1} - f^Q_{s_2}\right)\Big|_{(0,0)}, -\left(f^P_{s_1} - f^P_{s_2}\right)\Big|_{(1,1)}, -\left(f^Q_{s_1} - f^Q_{s_2}\right)\Big|_{(1,1)}. \tag{23}$$

Furthermore, we obtain $\Delta|_{(0,0)} > 0$, $\Delta|_{(1,1)} > 0$, $T|_{(0,0)} < 0$, and $T|_{(1,1)} < 0$. Therefore, both steady states of (0,0) and (1,1) are stable.

B. Fixed points (0,1) and (1,0)

For the fixed point (0,1), we have the following cases:

(1) (0,1) is stable if $\lambda_P < \lambda_P^{c_1}$ and $\lambda_Q < \lambda_Q^{c_1}$, since we have $\Delta|_{(0,1)} > 0$, $T|_{(0,1)} < 0$. Note that $\lambda_P^{c_1}$ and $\lambda_Q^{c_1}$ represent the critical values of coupling strength as defined by Eqs. (22).

(2) (0,1) is a saddle if $\lambda_P < \lambda_P^{c_1}, \lambda_Q > \lambda_Q^{c_1}$, or $\lambda_P > \lambda_P^{c_1}, \lambda_Q < \lambda_Q^{c_1}$ since both conditions leads to $\Delta|_{(0,1)} < 0$.

(3) (0,1) is unstable if $\lambda_P > \lambda_P^{c_1}, \lambda_Q > \lambda_Q^{c_1}$ since this leads to $\Delta|_{(0,1)} > 0$, $T|_{(0,1)} > 0$.

In a full analogy, we have the following cases for the fixed point (1,0):

(1) (1,0) is stable if $\lambda_P < \lambda_P^{c_2}$ and $\lambda_Q < \lambda_Q^{c_2}$, since $\Delta|_{(1,0)} > 0$, $T|_{(1,0)} < 0$. Again, $\lambda_P^{c_2}$ and $\lambda_Q^{c_2}$ are critical values of coupling strength.

(2) (1,0) is a saddle if $\lambda_P < \lambda_P^{c_2}, \lambda_Q > \lambda_Q^{c_2}$, or $\lambda_P > \lambda_P^{c_2}, \lambda_Q < \lambda_Q^{c_2}$ since both conditions leads to $\Delta|_{(1,0)} < 0$.

(3) (1,0) is unstable if $\lambda_P > \lambda_P^{c_2}, \lambda_Q > \lambda_Q^{c_2}$ since this leads to $\Delta|_{(1,0)} > 0$, $T|_{(1,0)} > 0$.

C. Quasisteady states

Again, we take $(x^L(0),0)$ as an example. We show that $\Delta|_{(x^L(0),0)} < 0$, since $0 < x^L(0) < 1$, $\lambda_P < \lambda_P^{c_2}$ and $(f^Q_{s_1} - f^Q_{s_2})|_{(x^L(0),0)}$. This shows that the fixed point $(x^L(0),0)$ is a saddle.

By the same procedure, we prove that quasi-steady states $(x^L(1),1)$, $(0,y^L(0))$ and $(1,y^L(1))$ are saddles.

D. Fixed point $(x^\sharp, y^\sharp)$

The intersection point by the nullclines $x^L(y)$, $y^L(x)$ [Eqs. (17), (18)] in the $(x-y)$ plane yields the fixed point

$(x^\sharp, y^\sharp)$ of the system. In particular, we have

$$x^\sharp = \frac{x^* + \lambda_P x^* - \lambda_P y^* - \lambda_P\lambda_Q y^*}{1-\lambda_P\lambda_Q}, \tag{24}$$

$$y^\sharp = \frac{y^* + \lambda_Q y^* - \lambda_Q x^* - \lambda_P\lambda_Q x^*}{1-\lambda_P\lambda_Q}. \tag{25}$$

Because of $0 \leqslant x^\sharp, y^\sharp \leqslant 1$, we obtain the existence conditions of $(x^\sharp, y^\sharp)$ as following:

$$\begin{aligned} &\max\left\{\frac{y^*}{x^*}, \frac{1-y^*}{1-x^*}\right\} < \frac{1+\lambda_P}{\lambda_P+\lambda_P\lambda_Q}, \\ &\max\left\{\frac{x^*}{y^*}, \frac{1-x^*}{1-y^*}\right\} < \frac{1+\lambda_Q}{\lambda_Q+\lambda_P\lambda_Q}, \end{aligned} \quad \text{if } \lambda_P\lambda_Q < 1, \tag{26}$$

$$\begin{aligned} &\min\left\{\frac{y^*}{x^*}, \frac{1-y^*}{1-x^*}\right\} > \frac{1+\lambda_P}{\lambda_P+\lambda_P\lambda_Q}, \\ &\min\left\{\frac{x^*}{y^*}, \frac{1-x^*}{1-y^*}\right\} > \frac{1+\lambda_Q}{\lambda_Q+\lambda_P\lambda_Q}, \end{aligned} \quad \text{if } \lambda_P\lambda_Q > 1. \tag{27}$$

With the notations of Eqs. (15), the above existence conditions [Eqs. (26) and (27)] are simplified as

$$\lambda^{c_1} < \varepsilon_1, \varepsilon_2 < \lambda^{c_2}, \quad \lambda_P\lambda_Q < 1, \tag{28}$$

$$\lambda^{c_2} < \varepsilon_1, \varepsilon_2 < \lambda^{c_1}, \quad \lambda_P\lambda_Q > 1, \tag{29}$$

where

$$\lambda^{c_1} = \frac{\lambda_Q + \lambda_P\lambda_Q}{1+\lambda_Q}, \quad \lambda^{c_2} = \frac{1+\lambda_P}{\lambda_P+\lambda_P\lambda_Q}. \tag{30}$$

Therefore, we distinguish the following three cases:

(1) $(x^\sharp, y^\sharp)$ exists for both weak $(\lambda_P, \lambda_Q \ll 1)$ and strong couplings $(\lambda_P, \lambda_Q \gg 1)$;

(2) $(x^\sharp, y^\sharp)$ does *not* exist if $\lambda_P\lambda_Q \approx 1$ because $\lambda^{c_1} \approx \lambda^{c_2} \approx 1$;

(3) The conditions [Eqs. (26) and (27)] become easily fulfilled when x^* is close to y^*.

Once the existence conditions are fulfilled, we have $T|_{(x^\sharp, y^\sharp)} > 0$, which further suggests the stability of the steady state $(x^\sharp, y^\sharp)$ as follows:

(1) If $\lambda_P\lambda_Q < 1$, $(x^\sharp, y^\sharp)$ is unstable since $\Delta|_{(x^\sharp, y^\sharp)} > 0$.

(2) If $\lambda_P\lambda_Q > 1$, $(x^\sharp, y^\sharp)$ is a saddle since $\Delta|_{(x^\sharp, y^\sharp)} < 0$.

In summary, the system has parameters $\mathbf{A}_P, \mathbf{A}_Q, \lambda_P$, and λ_Q, which make bifurcation analysis complicated. Nevertheless, the fixed points and their corresponding stability properties are summarized in the following (as schematically shown in Figs. 1 and 2):

(1) (0,0) and (1,1) always exist and are stable.

(2) (0,1) is stable if the conditions (i) $\lambda_P < \lambda_P^{c_1}$ *and* (ii) $\lambda_Q < \lambda_Q^{c_1}$ are fulfilled. (0,1) is unstable if either (i) or (ii) is not fulfilled [see the areas delineated by horizontal and vertical dashed lines in Fig. 1(a)].

(3) Similarly, (1,0) is stable if the conditions (iii) $\lambda_P < \lambda_P^{c_2}$ *and* (iv) $\lambda_Q < \lambda_Q^{c_2}$ are fulfilled. (1,0) is unstable if either (iii) or (iv) is not fulfilled [see the areas delineated by horizontal and vertical dashed lines Fig. 1(b)].

(4) $(x^L(0), 0)$, $(x^L(1), 1)$, $(0, y^L(0))$, and $(1, y^L(1))$ are saddles when they exist (see the areas filled with diagonal continuous lines in Fig. 1).

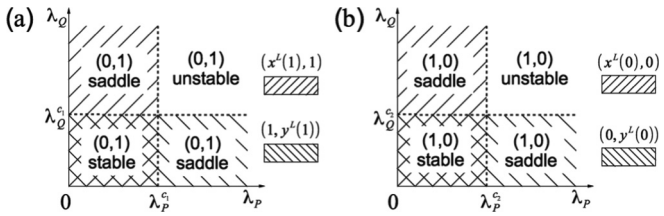

FIG. 1. Illustrations of the bifurcation diagrams in (λ_P, λ_Q). Note that (0,0) and (1,1) always exist and are stable. (a) Fixed point (0,1) is stable in the area of $\lambda_P < \lambda_P^{c_1}$ and $\lambda_Q < \lambda_Q^{c_1}$. The existence areas of fixed points (saddles) $(x^L(1), 1)$ and $(1, y^L(1))$ are filled with diagonal continuous lines as indicated by legends, respectively. (b) Fixed point (1,0) is stable in the area of $\lambda_P < \lambda_P^{c_2}$ and $\lambda_Q < \lambda_Q^{c_2}$. The existence areas of fixed points (saddles) $(x^L(0), 0)$ and $(0, y^L(0))$ are filled with diagonal continuous lines as indicated by legends, respectively.

(5) $(x^\sharp, y^\sharp)$ is unstable if the existence conditions [Eqs. (28) and (29)] are fulfilled (see Fig. 2).

V. NUMERICAL RESULTS

For numerical simulations, we first study the stabilities of fixed points in the corresponding phase space $[0,1] \times [0,1]$ in Sec. V A. Later, we choose parameter settings in such a way that P population is absorbed to all s_2 strategies ($x = 0$) and study the coupling effects λ_Q on the fixation probability p_Q of Q population in Secs. V B, V C. Finally, we show that our results hold for a wide range of selection strength β. To this end, we focus on the payoff matrices

$$\mathbf{A}_P = \begin{pmatrix} 1.2 & 0 \\ 0.8 & 1 \end{pmatrix}, \quad \mathbf{A}_Q = \begin{pmatrix} 1.4 & 0 \\ 0.5 & 1 \end{pmatrix}. \tag{31}$$

The selection strength $\beta = 100$ and population size is $N = 1000$. According to the definitions by Eqs. (22), we have $\lambda_P^{c_1} = 2.5$, $\lambda_Q^{c_1} = 0.9$, $\lambda_P^{c_2} = 0.4$, $\lambda_Q^{c_2} = 10/9$. Furthermore, $x^* = 0.71$, $y^* = 0.53$. We note that the bifurcation scenarios below do not depend on the particular values of the payoff matrices once the conditions of coordination games are fulfilled.

A. Phase space partitions

We start the simulations when the fixed points (1,0) and (0,1) are stable, plus the other two always-stable points (0,0) and (1,1). For convenience, these four stable states are denoted by $\Phi_{00} = (0,0)$, $\Phi_{10} = (1,0)$, $\Phi_{01} = (0,1)$, $\Phi_{11} =$

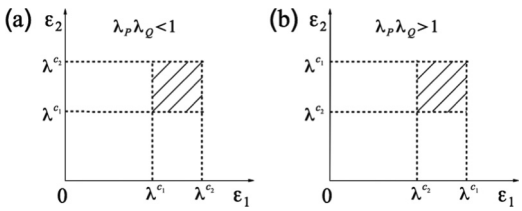

FIG. 2. Schematic illustrations of the existence conditions [Eqs. (28) and (29)] of the unstable fixed point $(x^\sharp, y^\sharp)$ in the parameter space of $(\varepsilon_1, \varepsilon_2)$, where $\lambda^{c_1}, \lambda^{c_2}$ are defined by Eq. (30). (a) $\lambda_P\lambda_Q < 1$ and (b) $\lambda_P\lambda_Q > 1$.

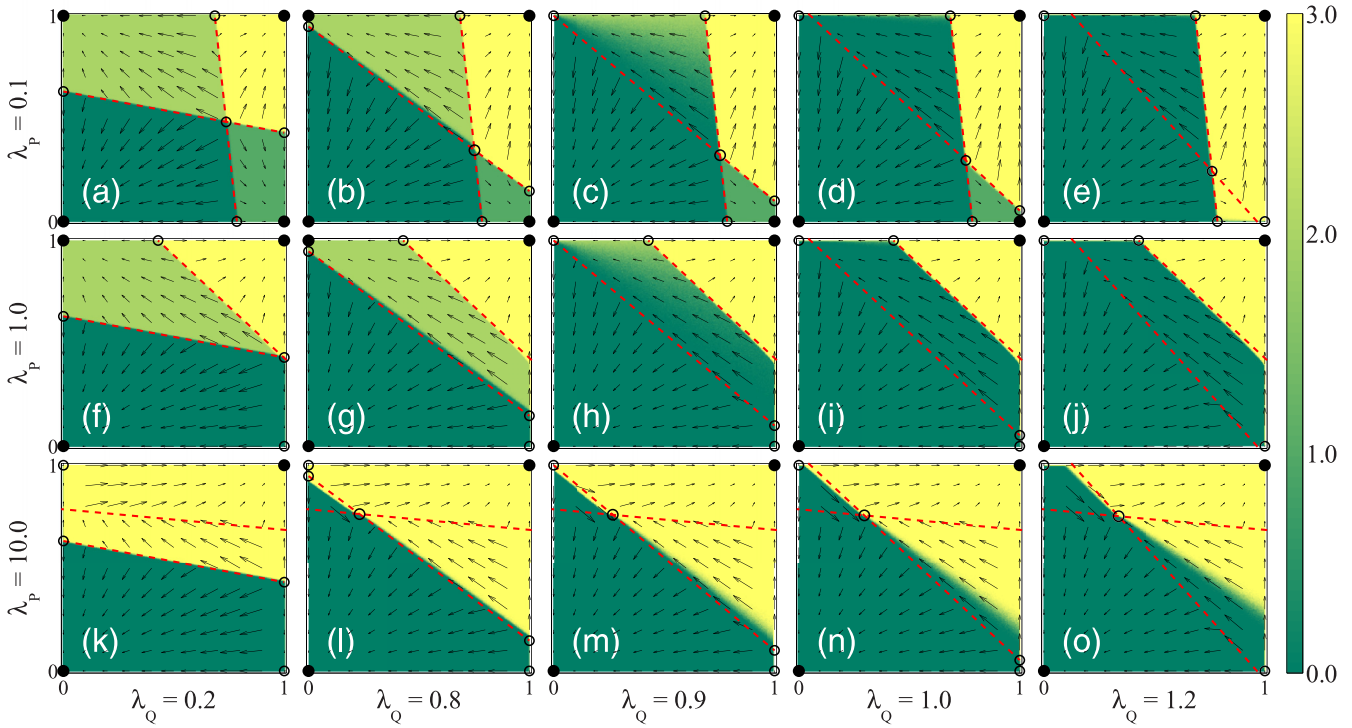

FIG. 3. Phase space depending on different coupling strength between two groups P and Q. Dashed lines are nullclines $x^L(y)$ and $y^L(x)$. The velocity field is indicated by the arrows, showing the direction of evolution. Stable fixed points are denoted by filled dots, while unstable ones are represented by open circles. The relationship between Ψ and each stable state is the following: $\Psi = 0$ means that the system is attracted to Φ_{00} with probability 1 (dark green); $\Psi = 1$ means that the system is attracted to Φ_{10} with probability 1 (green); $\Psi = 2$ means that the system is attracted to Φ_{01} with probability 1 (light green); and $\Psi = 3$ means that the system is absorbed into Φ_{11} with probability 1 (yellow).

(1,1), respectively. Starting from any pair of initial condition (x_0, y_0), the system reaches one of the state Φ_i with probability p_i,($\sum p_i = 1, i = [1,4]$). We further introduce a global variable $\Psi = 0p_1 + 1p_2 + 2p_3 + 3p_4$, which helps the color coding to separate the basin of attractions as shown in Fig. 3.

The results are summarized in the following:

(1) Small coupling $\lambda_P = 0.1$ [Figs. 3(a)–3(e)].

(a) For small coupling $\lambda_Q = 0.2$, there are nine fixed points. Starting from any pair of initial condition (x_0, y_0), the system is attracted to one of the stable state ϕ_i. When λ_Q is increased to $\lambda_Q = 0.8 < \lambda_Q^{c_1}$, the y nullcline $y^L(x)$ rotates around $(x^\sharp, y^\sharp)$ in a clockwise direction, changing the basins of attraction to the respective stable steady states.

(b) When λ_Q is increased to$\lambda_Q^{c_1} = 0.9$, the y nullcline crosses (0,1), leading that (0,1) is at a critical stage. Interestingly, we find that the basin of attraction to (0,1) is significantly decreased due to the change of group interaction. Namely, the critical fixation probability of population Q to all s_1 strategies is significantly increased (delayed). We will discuss about this process in more detail.

(c) When λ_Q is increased to 1.0 (larger than $\lambda_Q^{c_1}$), the point (0,1) becomes a saddle and $(0, y^L(0)$ disappears. Except the absorbing state $(x_0, y_0) = (0,1)$, all initial conditions in the region $(x_0, y_0) = [0, x^L(y_0)] \times [0,1)$ are attracted to the absorbing state Φ_{00}.

(d) When λ_Q is further increased to 1.2, the point (1,0) becomes a saddle, too. All initial conditions in the region $(x_0, y_0) = (x^L(y_0), 1) \times (0,1)$ are attracted to the absorbing state Φ_{11}.

(2) Intermediate coupling $\lambda_P = 1.0 > \lambda_P^{c_2}$ [Figs. 3(f)–3(j)].

(a) When $\lambda_Q = 0.2$, the x-nullcline crosses (1,0) and the point (1,0) is a saddle.

(b) When $\lambda_Q = 0.8$, the point $(x^\sharp, y^\sharp)$ does *not* exist. The phase space is divided into three regimes by nullclines $x^L(y), y^L(x)$, representing three absorbing states Φ_{00}, Φ_{01}, and Φ_{11} respectively.

(c) When $\lambda_Q = 1.0 > \lambda_Q^{c_1}$, the point (0,1) becomes a saddle. All initial conditions in the region $(x_0, y_0) = [0,1) \times [0, y^L(x_0))$ are attracted to the absorbing state Φ_{00}, except the absorbing state $(x_0, y_0) = (0,1)$.

(d) When λ_Q is further increased to 1.2, the point (1,0) keeps to be unstable.

(3) Strong coupling $\lambda_P = 10.0 > \lambda_P^{c_1}$ [Figs. 3(k)–3(o)].

(a) When $\lambda_Q = 0.2$, the fixed point (0,1) is a saddle before x nullcline $x^L(y)$ crosses (0,1). This means that there are only two stable fixed points (0,0) and (1,1).

(b) When λ_Q is increased to 0.8, the fixed point $(x^\sharp, y^\sharp)$ is newly created, which is a saddle.

(c) When λ_Q is further increased from 0.9 to 1.2, the y nullcline $y^L(x)$ rotates in the clockwise direction, showing similar scenarios as the case of Figs. 3(a)–3(e).

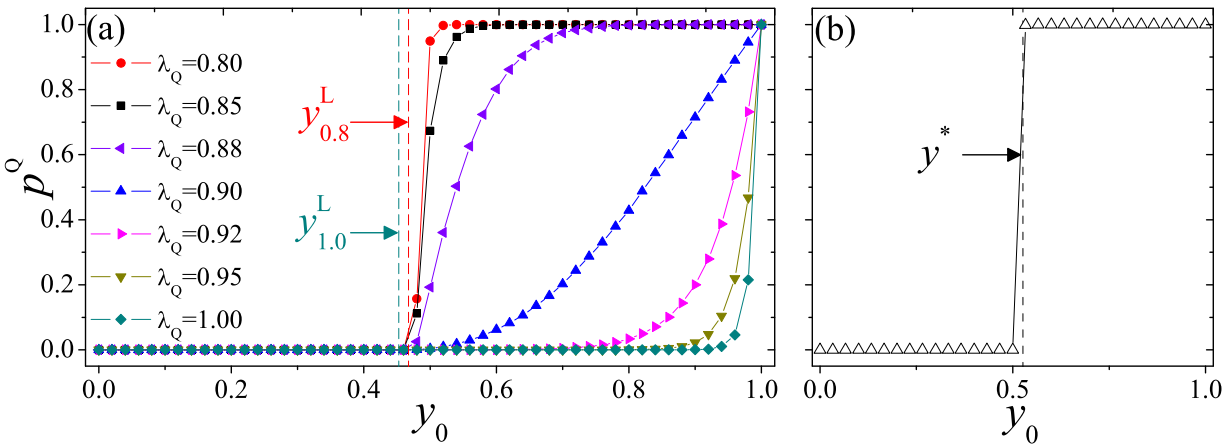

FIG. 4. Fixation probabilities p^Q to pure s_1 players (selection strength $\beta = 100$). (a) Effects of coupling strength λ_Q on p^Q. Legends are for various λ_Q values. The critical values of the unstable point $y^L_{\lambda_Q}(x_0 = 0.6, \lambda_Q = 0.8) \approx 0.47$, $y^L_{\lambda_Q}(x_0 = 0.6, \lambda_Q = 1.0) \approx 0.45$ (when P and Q are coupled) are highlighted by two vertical dashed lines. Each dot is an average over 1×10^5 random realizations. (b) Fixation probabilities for an isolated Q population, where an explosive transition is observed when $y_0 > y^* \approx 0.53$.

B. Red queen scenario

Next we choose the initial density of s_1 players in P population as $x_0 = 0.6$ and coupling strength $\lambda_P = 0.1$. Based on Eqs. (11) and (12), P group evolves to $x = 0$ for any initial conditions of population Q ($0 < y_0 < 1$) because of $F < 0$. By this initial settings for P population, we study the effect of coupling strength λ_Q on the fixation probability p^Q. The results are illustrated in Fig. 4(a). Taking $\lambda_Q = 0.8 < \lambda_Q^{c_1} = 0.9$ as an example, there is an unstable fixed point $y^L(x_0 = 0.6, \lambda_Q = 0.8) \approx 0.47$, which separates the absorbing state $y = 0$ from $y = 1$. Namely, above the critical density value 0.47, the Q population evolves toward 100% of s_1 individuals [4,10,28]. Furthermore, according to Eq. (18) we have $y^L(x_0) < y^*$ when λ_Q is introduced.

Comparing to the case when Q is decoupled with P [Fig. 4(b)], we find rather distinct scenarios of the fixation probabilities of p^Q for coupled populations (i.e., $\lambda_Q > 0.8$) as follows:

(1) When coupling strength λ_Q is increased from 0.8 to 1.0, p^Q is significantly decreased from 1 to 0. For instance, the fixed point $y^L_{\lambda_Q}(x_0 = 0.6, \lambda_Q = 0.8)$ is not able to clearly separate the two absorbing states. This is because the absorbing state $y = 1$ for the single population is *not* an attractor any more when λ_Q is present.

(2) When $y_0 > y^L(x_0)$, Q population shows a gradual continuous transition from one absorbing state $y = 0$ to the other $y = 1$. Namely, there are intermediate situations that Q group evolves to pure s_1 players only with some probabilities. In contrast, in a single Q population, there is an explosive jump in p^Q when the initial density $y_0 > y^*$ [Fig. 4(b)].

The explanations for the above two results are based on Eqs. (11) and (12). Population P evolves to $x = 0$ always since $F < 0$ for any $y_0 \in (0,1)$. For the Q population, we have two different cases: (i) For $y_0 < y^L(x_0)$, we have $G < 0$ such that Q evolves to $y = 0$. (ii) For $y_0 > y^L(x_0)$, we have $G > 0$ such that Q evolves to $y = 1$. The s_2 players in group Q get higher payoffs than that of s_1 players due to the coupling to P population, which changes G to be negative [Eqs. (12)]. Finally, the two populations evolves to Φ_{00}, namely, all players have s_2 strategy. Certainly, the P group has larger influences on players of Q group if the coupling strength λ_Q is larger, which increases the probability that the system is attracted to Φ_{00}.

There are significant evolutionary biological insights for the above findings. According to evolutionary dynamics of one single population, the mutant genes (say, of s_2 strategy) are not able to take over the whole Q population. However, when Q interacts with group P significantly (larger than some proper threshold λ_Q), the mutant genes may dominant the whole Q population although they still have small fitness within Q group. Our result supports the red queen hypothesis that the evolution of P population provides much pressure on the evolution of Q population due to the group interactions and interdependencies. So Q population has to evolve though the environment within Q is not ever-changed (i.e., the payoff matrix $\mathbf{A}_Q$ is unchanged). This scenario takes place if the coupling strength is larger than some threshold $\lambda_Q^{c_1}$.

Note that we find similar red queen dynamics for different coupling strength and initial density of s_1 players in P population, which are illustrated in Appendix B.

C. Decaying of s_1 strategy in population Q

Next, we compute the decaying (extinction) speed of the density of s_1 players in Q population, or equivalent to show how fast s_2 strategy takes over the entire Q population. For the ease of explanations, we again choose $x_0 = 0.6$ and $\lambda_P = 0.1$, which yields $x = 0$ (pure s_2 players) in P population. In other words, there is always a dying-out process for the s_1 strategy in the P population. When $\lambda_Q > \lambda_Q^{c_1}$, we find that p^Q decreases monotonically as shown in Fig. 5. Furthermore, p^Q decays faster if the initial number of s_2 players is larger in Q population. In other words, the probability that s_2 strategy takes over the Q population increases monotonically.

Based on Figs. 4 and 5, there are two competing timescales that are responsible for the change of the fixation probabilities p^Q. The first is the growing process of the density of s_1 strategy of Q population (i.e., dying-out of s_2 players). The second

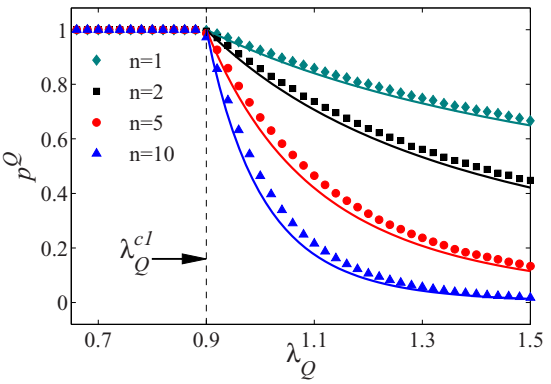

FIG. 5. Fixation probabilities p^Q versus coupling strength λ_Q in Q population. Parameter settings are the same as Fig. 4. Four cases of initial number of s_2 players in Q are denoted by $n = 1, 2, 5, 10$. The vertical dashed line corresponds to the critical coupling $\lambda_Q^{c_1} = 0.9$. Continuous lines are from the corresponding theoretical predictions [Eq. (38)].

timescale is the dying-out process of the density of s_1 players in the P population (i.e., growing of s_2 players). Starting from a given initial condition, the payoffs of s_2-players in Q population are smaller than that of s_1 strategy, which suggests that the frequency of s_2 players is decreased in Q. If there would be no coupling (i.e., isolated Q), the Q population reaches the absorbing state of all s_1 strategy ($y = 1$), which needs time T_Q. When Q is coupled with P, however, before reaching the absorbing state $y = 1$, there is an increasing number of s_2 players in P population who have larger payoffs than those s_2 players in Q, since P is attracted to all s_2 players.

More specifically, given the initial condition x_0 in P, we suppose it needs some time t' to reach the transient state of x', which reads

$$x' = \frac{C-A}{\lambda_Q(A+D-B-C)} + \frac{D-B}{A+D-B-C}, \quad \lambda_Q \geqslant \lambda_Q^{c_1}. \tag{32}$$

Again, x represents the frequency of s_1 players in the P population. Therefore, the Q population reaches the state of pure s_1 strategy ($y = 1$) if $T_Q < t'$. On the other hand, the Q population is occupied by pure s_2 players if $T_Q > t'$. In other words, the time scale for the dying-out phase of s_2 players in Q has to be longer than the average time that the P group reaches the absorbing state of $x = 0$ (pure s_2 players).

In the following, we compute the fixation probabilities of Q population to the state of pure s_1 players (i.e., s_2 strategy takes over the entire Q population). Let us denote $\theta(n,t)$ to be the probability that the Q population evolves to pure s_1 players in t time steps when initially n players having s_2 strategy (namely, density variable $y = 1 - n/N$ in Eq. (12)). In the same evolutionary time period t' (from the initial condition x_0 to x'), the fixation probabilities of Q population to pure s_1 strategy is given by

$$p^Q = \int_{t=0}^{t'} \theta(n,t)dt. \tag{33}$$

Further, we suppose the parameter $\beta \to \infty$ and we have $f_{s_1}^P \ll f_{s_2}^P$ and $f_{s_1}^Q \gg f_{s_2}^Q$. Equations (7)–(10) are approximated by

$$T_+^P \approx 0, \quad T_-^P \approx x \tag{34}$$

and

$$T_+^Q \approx 1 - y = \frac{n}{N}, \quad T_-^Q \approx 0. \tag{35}$$

When N is very large, we have

$$t' \approx N \int_{x_0}^{x'} \frac{1}{x} dx = N \ln \frac{x'}{x_0}, \tag{36}$$

and

$$\theta(n,t) = \sum_{t_{n-1}=n-1}^{t} \cdots \sum_{t_2=2}^{t_3} \sum_{t_1=1}^{t_2} \left(1 - \frac{1}{N}\right)^{t_1-1} \frac{1}{N} \left(1 - \frac{2}{N}\right)^{t_2-t_1-1} \times \frac{2}{N} \cdots \left(1 - \frac{n}{N}\right)^{t-t_{n-1}-1} \frac{n}{N}. \tag{37}$$

Substituting condition Eqs. (36) and (37) into Eq. (33), we have

$$p^Q \approx \left(1 - \frac{x'}{x_0}\right)^n, \tag{38}$$

since $\lim_{x\to\infty}(1 + \frac{1}{x})^x = e$ when $n \ll N$. This approximation suggests that the fixation probabilities p^Q decays exponentially when the number of s_2 players is increased, provided the

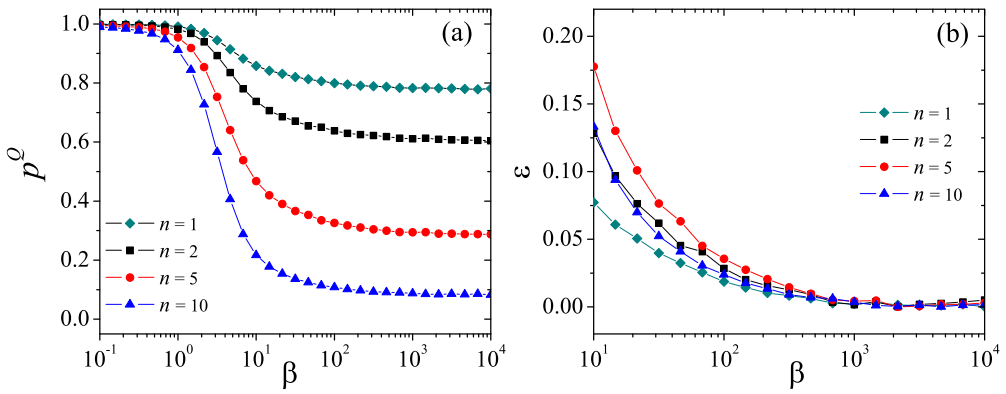

FIG. 6. Effects of selection strength β on the estimation of fixation probabilities p^Q [Eq. (38)]. The parameters are the same as described in the caption of Fig. 5, besides $\lambda_Q = 1.2$. (a) p^Q vs. β for various initial number of s_2 players in Q population. (b) Estimation errors.

coupling $\lambda_Q > \lambda_Q^{c_1}$ and $x_0 < x^L(y)$. The numerical simulation has confirmed this theoretical prediction as shown in Fig. 5.

Note that the above considerations in obtaining Eq. (38) are based on large selection strength $\beta \to \infty$. We verify that this result holds for a rather large interval of β as shown in Fig. 6. We further compute the estimation errors between the numerical simulation and Eq. (38), which is denoted by ε. The estimation errors are approximately smaller than 0.05 if $\beta > 50$ [Fig. 6(b)]. Therefore, our results do not depend much on the selection parameter β.

VI. CONCLUSIONS

In general, when two populations interact with each other, nontrivial coevolutionary dynamics will take place in many different contexts. We generalize coordination game model from one to two interacting populations, focusing on the effects of coupling strength to the dynamic process. We perform a systematic analysis for this model under the well-mixing limit and obtain all fixed points and their corresponding existence and stability conditions, which have been summarized in Sec. IV.

We have demonstrated that the interaction strength between two populations crucially alter the dynamic behavior, as shown by the corresponding phase space $[0,1] \times [0,1]$ (Fig. 3). More specifically, in a single population of two strategies s_1 and s_2, the whole population is attracted to all s_1 players if the initial density x_0 of s_1 players is larger than x^* ($x_0 > x^*$). The variants of low density $(1 - x_0)$ die out. Furthermore, the fixation probability shows an explosive transition from $x = 0$ to $x = 1$ at x^* as predicted by the replicator equation [Fig. 4(b)]. However, when coupling strength is introduced between two populations, this critical initial density x^* corresponding to fixation is significantly delayed if the coupling strength is larger than some threshold value. In contrast, the two populations evolve to the opposite state of pure s_2 players, which are in favor of the red queen hypothesis. The very few variants in one population can take over the whole population before dying out due to the higher payoffs they get from the other population, when coupling strength is sufficiently strong. We delineate the extinction time of strategy s_1 explicitly (or equivalent to the growing time of strategy s_2), which is an exponential form.

In our game models on interacted populations, we focused on well-mixing limit only. Note that further work will consider effects of under-dominance [36,37], migration between divided populations [38,39], and correlated dynamics of strategy updating rules with structure variation of populations [43]. Coupled populations of different sizes $N_P \neq N_Q$ may introduce cooperation pressure and strategy correlations to the system [42]. More specifically, we need to introduce a new parameter $\alpha = N_P/N_Q$ in the payoffs [Eqs. (3) and (4)]. The transition probabilities [Eqs. (5)–(10)] and the two-dimensional replicator Eqs. (11) and (12) do not change their functional forms. However, the fixed points and their respective stability conditions become more challenging since α affects all the following analysis. Furthermore, we focused on the Moran process only. The extension to other dynamic processes is a subject of future work, including pairwise payoff comparison [5,28], or even a mixture of both updating rules [44]. Nevertheless, we expect that much more complicated dynamic scenarios will appear in these different contexts.

ACKNOWLEDGMENTS

This work is financially supported by the National Natural Science of China (Grants No. 11305062 and No. 11405059).

APPENDIX A: JACOBIAN MATRIX

Here we provide the details for the Jacobian matrix for all nine fixed points.

Note that $\eta_i, i = 1, \ldots, 6$ are defined as

$$\eta_1 = \frac{df^P_{s_1}}{du^P_{s_1}}|_{(x^L(0),0)} = \frac{df^P_{s_2}}{du^P_{s_2}}|_{(x^L(0),0)},$$
$$\eta_2 = \frac{df^P_{s_1}}{du^P_{s_1}}|_{(x^L(1),1)} = \frac{df^P_{s_2}}{du^P_{s_2}}|_{(x^L(1),1)}, \tag{A1}$$

$$\eta_3 = \frac{df^Q_{s_1}}{du^Q_{s_1}}|_{(0,y^L(0))} = \frac{df^Q_{s_2}}{du^Q_{s_2}}|_{(0,y^L(0))},$$
$$\eta_4 = \frac{df^Q_{s_1}}{du^Q_{s_1}}|_{(1,y^L(1))} = \frac{df^Q_{s_2}}{du^Q_{s_2}}|_{(1,y^L(1))}, \tag{A2}$$

$$\eta_5 = \frac{df^P_{s_1}}{du^P_{s_1}}|_{(x^\sharp,y^\sharp)} = \frac{df^P_{s_2}}{du^P_{s_2}}|_{(x^\sharp,y^\sharp)},$$
$$\eta_6 = \frac{df^Q_{s_1}}{du^Q_{s_1}}|_{(x^\sharp,y^\sharp)} = \frac{df^Q_{s_2}}{du^Q_{s_2}}|_{(x^\sharp,y^\sharp)}. \tag{A3}$$

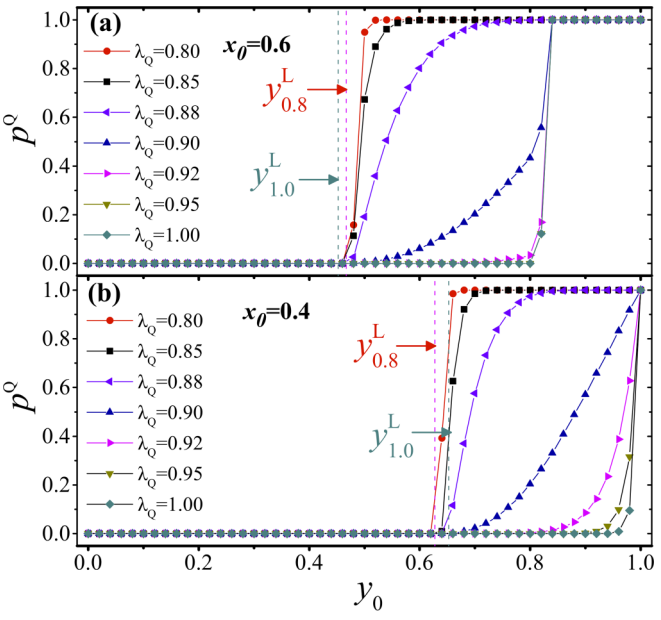

FIG. 7. Fixation probabilities p^Q to pure s_1 players in Q population for various coupling strength λ_Q as indicated by legends. (a) The initial density of s_1 players in P population is $x_0 = 0.6$. The critical values of the unstable point $y^L_{\lambda_Q}(x_0 = 0.6, \lambda_Q = 0.8) \approx 0.47$, $y^L_{\lambda_Q}(x_0 = 0.6, \lambda_Q = 1.0) \approx 0.45$ are highlighted by two vertical dashed lines. Each dot is an average over 1×10^5 random realizations. (b) The same as (a) but the initial density of s_1 players in P population is $x_0 = 0.4$.

We have $\eta_i > 0, i = 1, \ldots, 6$, since fitness are monotonic increasing functions of payoffs.

APPENDIX B: RED QUEEN DYNAMICS FOR $\lambda_P = 1$

We show that the red queen dynamics has been observed for different coupling strength $\lambda_P = 1.0$ and initial density of s_1 players in P population (shown in Fig. 7). For instance, if the initial density of s_1-players in P population is chosen as $x_0 = 0.6$, the critical fixation probability for Q population is significantly delayed [Fig. 7(a)]. According to Eq. (17), we have $x^L(y) = x^* + \lambda_P(x^* - y)|_{x_0=0.6}$. When $y_0 < 0.828$, P is absorbed to the state $x = 0$ (all s_2 players), since $F < 0$ [Eq. (11)]. On the other hand, if $y_0 > 0.828$, P population is attracted to the state $x = 1$ (all s_1 players) since $F > 0$. Due to the transition from $x = 0$ to $x = 1$ at $y_0 \approx 0.828$ in P population, Q population evolves to the state of all s_1 players since $G > 0$ [Eq. (12)]. Note, however, that if x_0 is chosen as 0.4, P group is attracted to zero density of s_1 players ($x = 0$) for any $y_0 \in (0,1)$. The result of Fig. 7(b) shows similar dynamic behavior as Fig. 4.

[1] J. M. Smith, *Evolution and the Theory of Games* (Cambridge University Press, Cambridge, England, 1982).
[2] J. Hofbauer and K. Sigmund, *Evolutionary Games and Population Dynamics* (Cambridge University Press, Cambridge, England, 1998).
[3] M. A. Nowak, A. Sasaki, C. Taylor, and D. Fudenberg, Nature **428**, 646 (2004).
[4] C. Taylor, D. Fudenberg, A. Sasaki, and M. A. Nowak, Bull. Math. Biol. **66**, 1621 (2004).
[5] A. Traulsen and C. Hauert, in *Reviews of Nonlinear Dynamics and Complexity*, edited by H.-G. Schuster (Wiley-VCH Verlag GmbH & Co. KGaA, Weinheim, Germany, 2009), Vol. 2, pp. 25–61.
[6] G. Szabó and G. Fáth, Phys. Rep. **446**, 97 (2007).
[7] A. Arenas, A. Díaz-Guilera, J. Kurths, Y. Moreno, and C. S. Zhou, Phys. Rep. **469**, 93 (2008).
[8] N. van Kampen, *Stochastic Processes in Physics and Chemistry, 3rd ed.* (Elsevier, Amsterdam, 2007).
[9] A. Traulsen, J. C. Claussen, and C. Hauert, Phys. Rev. Lett. **95**, 238701 (2005).
[10] A. Traulsen, M. A. Nowak, and J. M. Pacheco, Phys. Rev. E **74**, 011909 (2006).
[11] M. Mobilia, Phys. Rev. E **86**, 011134 (2012).
[12] M. Assaf and M. Mobilia, J. Stat. Mech.: Theory Experiment (2010) P09009.
[13] M. Assaf, M. Mobilia, and E. Roberts, Phys. Rev. Lett. **111**, 238101 (2013).
[14] A. J. Black, A. Traulsen, and T. Galla, Phys. Rev. Lett. **109**, 028101 (2012).
[15] A. Traulsen, J. C. Claussen, and C. Hauert, Phys. Rev. E **85**, 041901 (2012).
[16] T. Antal and I. Scheuring, Bull. Math. Biol. **68**, 1923 (2006).
[17] D. Zhou and H. Qian, Phys. Rev. E **84**, 031907 (2011).
[18] T. Galla, J. Theor. Biol. **269**, 46 (2011).
[19] B. Wu, P. M. Altrock, L. Wang, and A. Traulsen, Phys. Rev. E **82**, 046106 (2010).
[20] P. M. Altrock, A. Traulsen, and T. Galla, J. Theor. Biol. **311**, 94 (2012).
[21] J. Du, B. Wu, P. M. Altrock, and L. Wang, J. R. Soc. Interface **11**, 20140077 (2014).
[22] T. Antal, S. Redner, and V. Sood, Phys. Rev. Lett. **96**, 188104 (2006).
[23] K. Hashimoto and K. Aihara, J. Theor. Biol. **258**, 637 (2009).
[24] L.-X. Zhong, D.-F. Zheng, B. Zheng, C. Xu, and P. M. Hui, Europhys. Lett. **76**, 724 (2006).
[25] L. Cao, H. Ohtsuki, B. Wang, and K. Aihara, J. Theor. Biol. **272**, 8 (2011).
[26] F. Fu and M. A. Nowak, J. Stat. Phys. **151**, 637 (2013).
[27] K. H. Z. So, H. Ohtsuki, and T. Kato, J. Stat. Mech.: Theory Experiment (2014) P10020.
[28] L. Y. Zhang, Y. Zou, S. G. Guan, and Z. H. Liu, Phys. Rev. E **91**, 042807 (2015).
[29] S. Boccaletti, G. Bianconi, R. Criado, C. del Genio, J. Gmez-Gardees, M. Romance, I. Sendia-Nadal, Z. Wang, and M. Zanin, Phys. Rep. **544**, 1 (2014).
[30] L. van Valen, Evolutionary Theory **1**, 1 (1973).
[31] M. J. Benton, Science **323**, 728 (2009).
[32] K. L. Voje, Ø. H. Holen, L. H. Liow, and N. C. Stenseth, Proc. R. Soc. London B: Biol. Sci. **282**, 20150186 (2015).
[33] J. Gómez-Gardeñes, C. Gracia-Lázaro, L. M. Floria, and Y. Moreno, Phys. Rev. E **86**, 056113 (2012).
[34] Z. Wang, A. Szolnoki, and M. Perc, Europhys. Lett. **97**, 48001 (2012).
[35] M. D. Santos, S. N. Dorogovtsev, and J. F. F. Mendes, Sci. Rep. **4**, 4436 (2014).
[36] P. M. Altrock, A. Traulsen, and F. A. Reed, PLoS Comput. Biol. **7**, e1002260 (2011).
[37] P. M. Altrock, A. Traulsen, R. G. Reeves, and F. A. Reed, J. Theor. Biol. **267**, 62 (2010).
[38] P. Lombardo, A. Gambassi, and L. Dall'Asta, Phys. Rev. Lett. **112**, 148101 (2014).
[39] P. Lombardo, A. Gambassi, and L. Dall'Asta, Phys. Rev. E **91**, 032130 (2015).
[40] A. Traulsen, N. Shoresh, and M. A. Nowak, Bull. Math. Biol. **70**, 1410 (2008).
[41] P. M. Altrock and A. Traulsen, Phys. Rev. E **80**, 011909 (2009).
[42] T. Galla, Philos. Mag. **92**, 324 (2012).
[43] C.-B. Tang, B. Wu, J.-B. Wang, and X. Li, Sci. Rep. **4**, 4590 (2014).
[44] X. Liu, Q. Pan, Y. Kang, and M. He, J. Theor. Biol. **364**, 242 (2015).